2008-08-18

Bellman Pseudospectral Method

Ross, I. Michael

The American Institute of Aeronautics and Astronautics (AIAA)

AIAA/AAS Astrodynamics Specialist Conference and Exhibit
18 - 21 August 2008, Honolulu, Hawaii

AIAA 2008-6448

The Bellman Pseudospectral Method

I. Michael Ross,* Qi Gong,† Pooya Sekhavat‡

Based on the discoveries of a recently proposed algorithm for low-thrust trajectory optimization, we present the Bellman pseudospectral (PS) method for a generic optimal control problem. In our original algorithm, we combined the properties of PS methods with Bellman's principle to provide an optimal solution to multi-scale and long-horizon trajectory optimization problems. In this paper, we generalize this concept to provide a low cost solution to generate feasible solutions to optimal control problems. In the limit, this algorithm converges to our original concept; hence, our current proposal may also be considered as a cheap mesh-refinement technique for trajectory optimization in contrast to the more expensive PS knotting method. To facilitate the generalizations, we replace the convergence requirements in our original algorithm to controllability arguments. An application of the Bellman PS algorithm to an attitude control problem shows that the algorithm compares favorably to the PS knotting method.

I. Introduction

Over the last decade, pseudospectral (PS) methods have moved rapidly from a popular technique to flight implementation onboard the International Space Station as described recently in a front page story of *SIAM News*.[1] Thanks to the popularity of software packages such as OTIS[2] and DIDO,[3] PS methods are now used quite routinely within the aerospace community.[4−17]

In recent years, PS methods have been employed for advancing research on real-time optimal control. For closed-loop applications, accuracy and computational time are two crucial factors.[18,19] High accuracy is usually associated with a high computational cost because of the expectation of a fine mesh. Thus, an ongoing research topic is ways and means to balance these two requirements. Recently, Gong et al[20] proposed an autonomous mesh refinement technique based on the PS knotting method of Ross and Fahroo.[22] They showed that by choosing a mesh in a specially designed sequence, high fidelity solutions can be obtained at a moderate computational cost. In this paper, we propose an alternative approach. Instead of getting a very accurate *optimal* solution, we propose to provide *feasible* control signals at a very low computational cost. That is, in this paper we focus more on feasibility and computational cost by trading off on some optimality. Theoretically, if we insist on no-trades on optimality, then our algorithm "converges" to a first-principles application of Bellman's Principle of Optimality; hence, we refer to this approach as the Bellman PS method. Because the Bellman PS method is capable of generating feasible solutions in real time even for complex systems, it allows us to implement feedback solutions. These solutions can range from near optimal to merely feasible; however, by exploiting some additional properties of PS methods, it is possible to control the "degree" of optimality.

We note that the Bellman PS method is based on the recent discoveries of Ref. [21]. While the motivation and application in Ref. [21] was low-thrust trajectory optimization, in this paper, we show that the Bellman PS method can be applied to a generic optimal control problem whether or not "anti-aliasing" is sought. In Ref. [21], a theoretical justification for the approach is based on a convergence hypothesis for a low-order discrete solution, whereas in this paper we replace this assumption by a weaker one related to controllability of the original optimal control problem. Thus, the algorithm directly facilitates a closed-loop real-time implementation of PS methods, since a low computational cost directly affects the stability of the resulting

*Professor, Department of Mechanical and Astronautical Engineering, Naval Postgraduate School, Monterey, CA, E-mail: imross@nps.edu. Associate Fellow, AIAA.

†Assistant Professor, Department of Applied Mathematics and Statistics, University of California, Santa Cruz, CA, E-mail: qigong@soe.ucsc.edu.

‡Research Scientist, Department of Mechanical and Astronautical Engineering, Naval Postgraduate School, Monterey, CA E-mail: psekhava@nps.edu.

closed-loop system.[18,19] In its open-loop mode, the proposed algorithm may also be considered as a mesh-refinement technique for trajectory optimization. This concept is sharply different from the PS knotting method which relies on more traditional principles. In this paper, we show that Bellman PS method is capable of locating discontinuities in controls even when the number of PS nodes are low. We demonstrate this concept by applying both the Bellman PS method and the PS knotting method for the attitude control of NPSAT1, a spacecraft conceived, designed and built at the Naval Postgraduate School and scheduled to be launched in Fall 2009.

II. A Quick Background on Pseudospectral Methods

The key to modern computational optimal control is the approximation of function/trajectory. Given an arbitrary function $y(t)$, in PS methods, $y(t)$ is approximated by a polynomial $y^N(t)$ as

$$y(t) \approx y^N(t) = \sum_{j=0}^{N} \frac{W(t)}{W(t_j)} \phi_j(t) y_j, \ a \leq t \leq b$$

where the nodes $t_j, j = 0, ..., N$ are a set of distinct interpolation nodes (defined later) on the interval of interest, $W(t)$ is the weight function on the interval, and $\phi_j(t)$ is the $Nth-$ order Lagrange interpolating polynomial that satisfies the Kronecker relationship $\phi_j(t_k) = \delta_{jk}$. This implies that

$$y_j = y^N(t_j), \ \ j = 0, ...N.$$

An expression for the Lagrange polynomial can be written as[23]

$$\phi_j(t) = \frac{g_N(t)}{g'_N(t_j)(t - t_j)}, \ g_N(t) = \prod_{j=0}^{N} (t - t_j).$$

One important tenant of PS approximations of functions is that differentiation of the approximated function can be performed by differentiation of the interpolating polynomial,

$$\frac{dy^N(t)}{dt} = \sum_{j=0}^{N} \frac{y_j}{W(t_j)} [W'(t)\phi_j(t) + W(t)\phi'_j]$$

Since only the values of the derivative at the nodes t_i are required for PS methods, we have,

$$\left.\frac{dy^N(t)}{dt}\right|_{t_i} = \sum_{j=0}^{N} \frac{y_j}{W(t_j)} [W'(t_i)\delta_{ij} + W(t_i)D_{ij}] = \sum_{j=0}^{N} D_{ij}[W] y_j$$

where we use $D_{ij}[W]$ as a shorthand notation for the W-weighted differentiation matrix,

$$D_{ij}[W] := \frac{[W'(t_i)\delta_{ij} + W(t_i)D_{ij}]}{W(t_j)}$$

and D_{ij} is usual unweighted differentiation matrix given by,

$$D_{ij} := \left.\frac{d\phi_j(t)}{dt}\right|_{t=t_i}$$

Thus, when $W(t) = 1$, we have

$$D_{ij}[1] = D_{ij}$$

From Eq. (1), the unweighted differentiation matrix, $D_{ij} = \phi'_j(t_i)$, has the form,

$$D_{ij} = \begin{cases} \dfrac{g'_N(t_i)}{g'_N(t_j)} \dfrac{1}{(t_i - t_j)}, & i \neq j \\ \\ \dfrac{g''_N(t_i)}{2g'_N(t_i)}, & i = j \end{cases}$$

The preceding equations are general representations for the derivative of Lagrange polynomials evaluated at arbitrary interpolation nodes. Thanks to Runge, it is well-known that an improper selection of the grid points can lead to disastrous consequences. In fact, a uniform distribution of grid points is the worst possible choice for polynomial interpolation and hence differentiation. On the other hand, the best possible choice of grid points for integration, differentiation and interpolation of functions are Gaussian quadrature points. Consequently, all PS methods use Gaussian quadrature points.

Let $\{P_N(t)\}$ be a sequence of polynomials orthogonal with respect to an appropriate inner product; and let $t_0 = -1 < t_1 < \cdots < t_N = 1$ be the nodes. There are three common types of Gaussian quadrature points:

1) zeros of $P_{N+1}(t)$	Gauss quadrature nodes,
2) the end points and the critical points of $P_{N+1}(t)$	Gauss-Lobatto nodes,
3) the left end point and the zeros of $P_{N+1}(t) - \frac{P_{N+1}(-1)}{P_N(-1)} P_N(t)$	Gauss-Radau nodes.

Fig.1 illustrates the distribution of these quadrature nodes used for Legendre PS methods. One distinctive

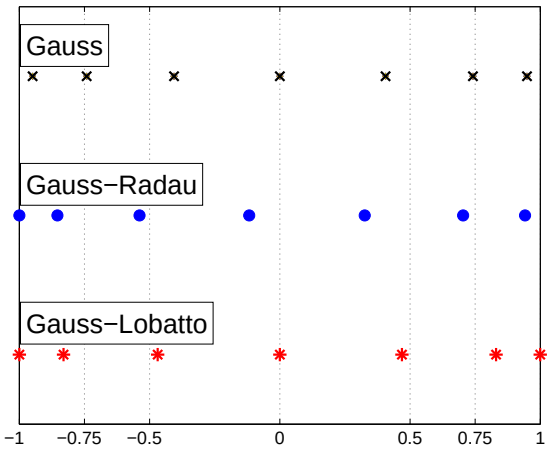

Figure 1. Illustration of quadrature points for Legendre PS methods.

feature of these nodes is their nonuniform distribution. The nodes are much more dense towards the end points. Indeed, the distance between the nodes converges at a rate of N^{-2} around end points[23,24] in contrast to N^{-1} convergence of uniform distribution. Later in this paper, we will utilize this key point to improve the quality of the solution.

Now, consider the following generic optimal control problem:

$$\begin{aligned} \text{Minimize} \quad J[x(\cdot), u(\cdot)] &= \frac{1}{2}\int_{-1}^{1} F(x(t), u(t))dt + E(x(-1), x(1)) \\ \text{Subject to} \quad \dot{x}(t) &= f(x(t), u(t)) \\ e(x(-1), x(1)) &= 0 \\ h(x(t), u(t)) &\leq 0 \end{aligned}$$

where $x \in \mathbb{R}^{N_x}, u \in \mathbb{R}^{N_u}, F : \mathbb{R}^{N_x} \times \mathbb{R}^{N_u} \to \mathbb{R}, E : \mathbb{R}^{N_x} \times \mathbb{R}^{N_x} \to \mathbb{R}, f : \mathbb{R}^{N_x} \times \mathbb{R}^{N_u} \to \mathbb{R}^{N_x}, e : \mathbb{R}^{N_x} \times \mathbb{R}^{N_x} \to \mathbb{R}^{N_e}, h : \mathbb{R}^{N_x} \times \mathbb{R}^{N_u} \to \mathbb{R}^{N_h}$.

Let $\bar{x}_k^N$ and $\bar{u}_k^N$ be an approximation of a feasible solution $(x(t), u(t))$ evaluated at the node t_k. Then, as a result of the discretization, the optimal control problem is transformed to a finite dimensional constrained nonlinear optimization problem. In the case of a Legendre PS method, this problem can be written as,

Problem $\mathbf{B^N}$: Find $\bar{x}_k^N$ and $\bar{u}_k^N$, $k = 0, 1, \ldots, N$, that minimize

$$\bar{J}^N(\bar{X}, \bar{U}) = \sum_{k=0}^{N} F(\bar{x}_k^N, \bar{u}_k^N) w_k + E(\bar{x}_0^N, \bar{x}_N^N)$$

subject to

$$\left\| D \begin{pmatrix} \bar{x}_{i0}^N \\ \vdots \\ \bar{x}_{iN}^N \end{pmatrix} - \begin{pmatrix} f_i(\bar{x}_0^N, \bar{u}_0^N) \\ \vdots \\ f_i(\bar{x}_N^N, \bar{u}_N^N) \end{pmatrix} \right\|_\infty \leq \delta_{1N}\mathbf{1} \quad i = 1, 2, \ldots, r-1$$

$$h(\bar{x}_k^N, \bar{u}_k^N) \leq \delta_{2N} \cdot \mathbf{1},$$

$$\left|\left| e(\bar{x}_0^N, \bar{x}_N^N) \right|\right|_\infty \leq \delta_{3N}$$

for all $0 \leq k \leq N$ where δ_{iN} is a given small number that depends upon N; see Ref. [20] for additional details.

The theoretical analysis carried out in Refs. [25–27] shows the well-posedness of PS discretization, i.e., preserving the feasibility of the original continuous problem and the consistency of the PS approximation[28] to the original optimal control problem. Problem B^N also satisfies dual consistency[27] which is exploited to generate a spectral algorithm[20] for solving a convergent sequence of discrete optimal control problems. A version of this algorithm is implemented in the software package, DIDO.[3]

III. Discrete-Time Vs Continuous-Time Feasibility

To validate a solution to a constrained optimal control problem, the most important criterion is feasibility. In PS methods, we distinguish two types of feasibilities: discrete-time and continuous-time feasibility.

When Problem B^N, is solved, the solution provides the value of the state and control at discrete nodes points. By definition, this solution satisfies all the discretized constraints, and is said to be discrete-time feasible. To obtain a valid solution to the original continuous-time optimal control problem, one needs to map the discrete solution to the continuous time domain. This is usually done by some kind of interpolation such as linear or spline. After such a mapping, the discrete-time feasible solution may not be feasible to the continuous-time problem. To illustrate this point, consider the following simple example:

$$\begin{cases} \text{Minimize} & J[x(\cdot), u(\cdot), t_f] = t_f \\ \text{Subject to} & \dot{x}_1 = x_2 \\ & \dot{x}_2 = u \\ & x(0) = [10, 10] \\ & x(t_f) = [0, 0] \\ & |u| \leq 1 \end{cases} \tag{1}$$

A 5-node PS solution to this problem is shown in Fig. 2. This solution is discrete-time feasible. Now, if we interpolate this 5-node discrete control using linear interpolation and propagate the control via the system dynamics, the trajectory is infeasible in the sense that the final condition ($x(t_f) = [0; 0]$) is not satisfied as illustrated in see Fig.3. One obvious solution to close the gap between the discrete-time and continuous-time feasibility is to increase the number of nodes. If Problem B^N is a consistent approximation[28] to Problem B, then, continuous-time feasibility can always be guaranteed for a sufficiently large number of nodes. A proof of this assertion for PS discretization is provided in Refs. [25, 27]. While increasing the number of nodes is a straightforward and a simple technique to eliminate the discrepancy between discrete-time and continuous-time feasibility, it is not necessarily the most efficient. In this paper, we propose an alternative approach to guarantee continuous-time feasibility. Our idea is based on Bellman's Principle of Optimality and its successful application to low-thrust trajectory optimization problems.[21]

IV. Bellman Pseudospectral Methods and Continuous-Time Feasibility

The discrepancy between discrete-time and continuous-time feasibility is due to the approximation error in the discretization and the interpolation. A simple way to reduce the error without increasing the number of nodes is based on a simple observation derived from Bellman's Principle.

Suppose we have a discrete-time feasible control, $\bar{u}_k^N$, $k = 0, 1, \ldots, N$ which generates a continuous-time trajectory, $t \mapsto x(t)$. Then, $\| \bar{x}_k^N - x(t_k) \|$, $k = 0, 1, \ldots, N$ denotes a measure of continuous-time feasibility. Now suppose that $\| \bar{x}_k^N - x(t_k) \|$ is small for $k = 0, 1, \ldots, N_s \ll N$, then, it is clear that if Problem B^N

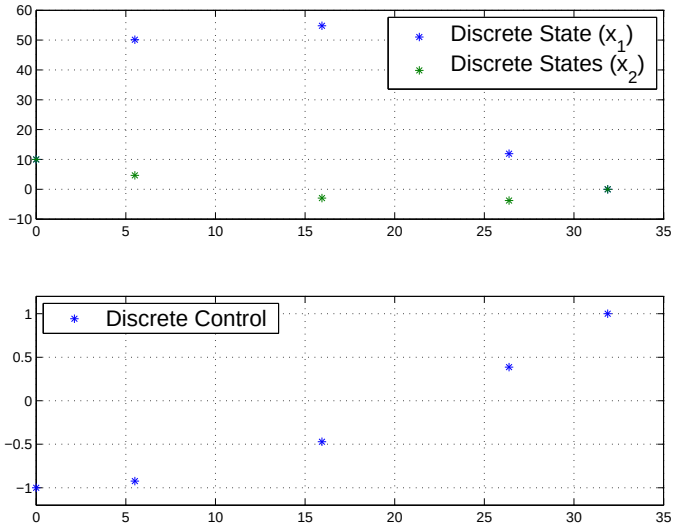

Figure 2. Discrete solution to Problem (1) with 5 nodes.

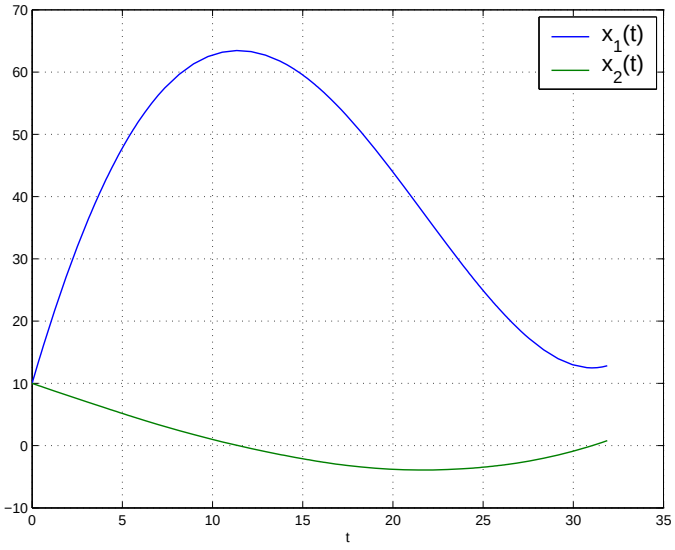

Figure 3. Propagated trajectory using linear interpolation of the 5-node discrete control.

were to be re-solved with $x(t_{N_s})$ as the initial condition, then a re-computation of the measure of infeasibility is reduced. By repeating this process, it is clear that we would have obtained a feasible solution to Problem B using very few number of nodes. A key assumption in the proposed concept is that the system must be controllable from each starting point, because if it not, then there is no N, no matter how large that will generate a continuous-time feasible solution. Of course, a rigorous mathematical analysis is needed to justify all these points.

To demonstrate the key point of improved feasibility, we apply this technique to Problem (1) using the halfway point as the initial point. The result is shown in Fig. 4. Compared to the trajectory in Fig. 3, it is apparent that continuous-time feasibility is significantly improved with just 5 nodes.

The idea is encapsulated in the following Bellman PS pseudocode:

1. Solve the optimal control problem using PS methods with N nodes;
2. Divide the time interval $[t_0, t_f]$ into m segments, $[t_i, t_{i+1}]$, and set $i = 0$;
3. Interpolate the discrete control and propagate the control to the end of the segment, t_{i+1};

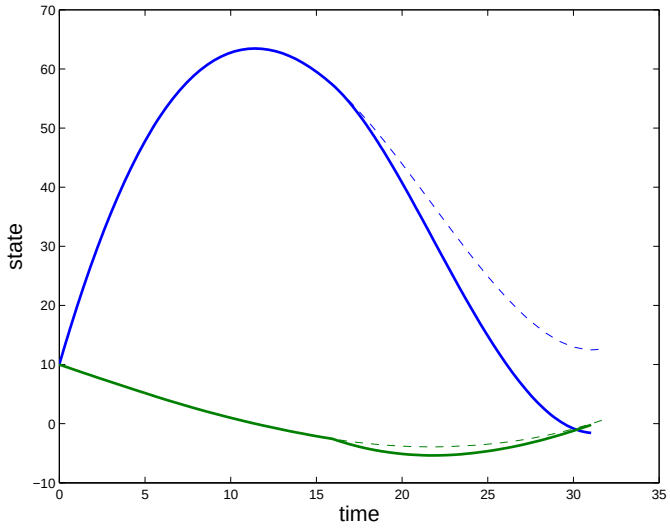

Figure 4. Solution to Problem (1) with 5 nodes. Solid lines are two-segment "Bellman" trajectories obtained by resolving the problem from the halfway point. Dashed lines are one-segment trajectories obtained by directly propagating the 5-node discrete control.

4. Use the propagated trajectory at t_{i+1} as a new initial condition and resolve the problem;
5. If $i = m - 1$, stop; else set $i = i + 1$ and go to step 3.

When the proposed method is applied for sufficiently large N, then under an appropriate proof of convergence, the error between the interpolation of discrete solution and continuous optimal solution is negligible. In such a case, the preceding algorithm is simply a demonstration of Bellman's Principle of Optimality. For low N, the resulting trajectory may not be optimal, but the algorithm will provide a feasible solution at a very low computational cost. The main reason for this is that, as the trajectory approaches the final point (assuming controllability), the distance traveled from the new initial condition to the final point will be small enough so that a continuous-time feasible solution can still be provided by a low number of nodes.

Remark 0.1 *In principle, the proposed algorithm can be applied to other discretization based methods; however because PS methods provide a very fast convergence rate, few nodes can provide high accuracy. More importantly, the dense distribution of nodes around initial point (see Fig.1) significantly reduces the interpolation error, since the control around initial period only is propagated.*

Remark 0.2 *For any given problem, a certain minimum number of nodes are necessary to successfully implement the algorithm. This is because reachability and controllability are not reversible; hence, it is possible that the discrete controller might place the state of the system into non-controllable regions. Thus, some conditions are necessary to ensure that the controller will not drive the trajectory further away from the final point.*

Remark 0.3 *If a sufficiently large number of nodes are used to implement the method, then it reduces to the algorithm proposed in Ref. [21], wherein we assumed that a low-N solution had indeed converged to the optimal solution and the technique was used for anti-aliasing purposes to capture the high-frequency components in the trajectory.*

Table 1 summarizes the results of applying the proposed algorithm to Problem 1. To measure the continuous-time feasibility, we use the end-point error,

$$Error \quad = \quad \sqrt{x_1(t_f)^2 + x_2(t_f)^2}$$

where $x_1(t)$ and $x_2(t)$ are the values of the propagated trajectory. The number of nodes used is 5 and m denotes the number of segments. Clearly, even with just 5 nodes, continuous-time feasibility can be significantly improved by simply increasing the number of segments. The trajectory with 10 segments is shown in Fig. 5.

m	$Error$
1	12.848
5	1.475
10	0.077
15	3.707e-004
20	2.914e-010

Table 1. Feasibility errors for Problem (1).

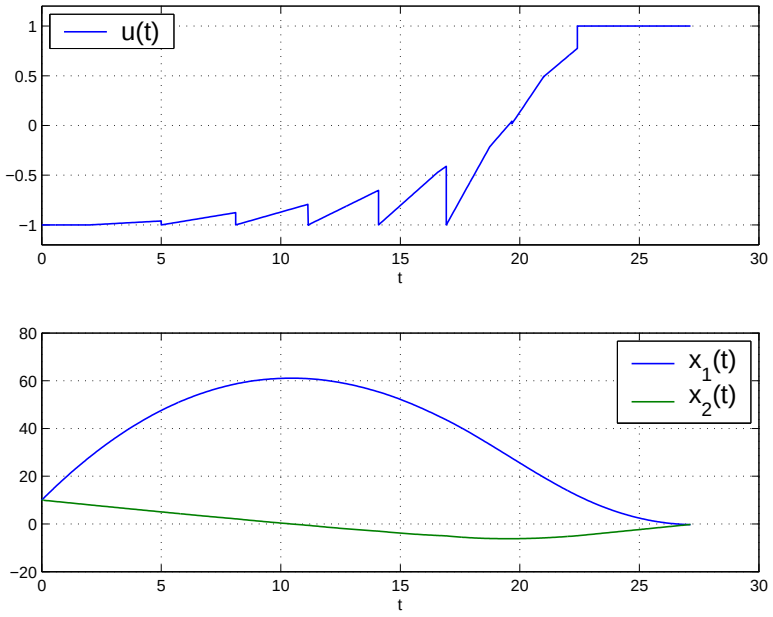

Figure 5. Bellman PS solution to Problem (1) with 5 nodes and 10 segments.

V. Bellman PS Method Vs Spectral PS Knotting Algorithm

To improve continuous-time feasibility, there are two possible approaches. One can either increase the number of nodes so that the error between the discrete and continuous solutions is negligible; or apply the proposed Bellman PS method. The increase in the number of nodes can be done quite efficiently and autonomously using the spectral algorithm.[20] By generating an efficient mesh, the accuracy of the discrete solution can be significantly improved. In this section, we compare the performance difference between these two methods on the NPSAT1 attitude control problem. An interesting characteristic of this problem is that the optimal control is discontinuous. To capture the switching points, in Ref.[20], the PS knotting method was combined with a mesh generating technique to obtain an accurate solution. In this section, we show that the proposed Bellman PS method can also capture the discontinuities but with a very few number of nodes.

NPSAT1 is a multi-purpose small satellite being built at the Naval Postgraduate School, and is scheduled to be launched in 2009. It is currently in its assembly stage. The spacecraft uses magnetic torque rods for attitude control. Detailed description of the spacecraft can be found in Ref.[18, 29]. Choosing the standard quaternion and body rates as the state variables, the dynamical equations of motion for NPSAT1 are given

by:[29]

$$
\begin{aligned}
\dot{q}_1(t) &= \frac{1}{2}\left[\omega_x(t)q_4(t) - \omega_y(t)q_3(t) + \omega_z(t)q_2(t) + \omega_0 q_3(t)\right] \\
\dot{q}_2(t) &= \frac{1}{2}\left[\omega_x(t)q_3(t) + \omega_y(t)q_4(t) - \omega_z(t)q_1(t) + \omega_0 q_4(t)\right] \\
\dot{q}_3(t) &= \frac{1}{2}\left[-\omega_x(t)q_2(t) + \omega_y(t)q_1(t) + \omega_z(t)q_4(t) - \omega_0 q_1(t)\right] \\
\dot{q}_4(t) &= \frac{1}{2}\left[-\omega_x(t)q_1(t) - \omega_y(t)q_2(t) - \omega_z(t)q_3(t) - \omega_0 q_2(t)\right] \\
\dot{\omega}_x(t) &= \frac{I_2 - I_3}{I_1}[\omega_y(t)\omega_z(t) - 3\frac{\mu}{r_0^3}C_{23}(q(t))C_{33}(q(t))] + \frac{1}{I_1}\left[B_z(q(t),t)u_2(t) - B_y(q(t),t)u_3(t)\right] \\
\dot{\omega}_y(t) &= \frac{I_3 - I_1}{I_2}[\omega_x(t)\omega_z(t) - 3\frac{\mu}{r_0^3}C_{13}(q(t))C_{33}(q(t))] + \frac{1}{I_2}\left[B_x(q(t),t)u_3(t) - B_z(q(t),t)u_1(t)\right] \\
\dot{\omega}_z(t) &= \frac{I_1 - I_2}{I_3}[\omega_x(t)\omega_y(t) - 3\frac{\mu}{r_0^3}C_{13}(q(t))C_{23}(q(t))] + \frac{1}{I_3}\left[B_y(q(t),t)u_1(t) - B_x(q(t),t)u_2(t)\right]
\end{aligned}
$$

where $\omega_0 = 0.00108 rad/s$ is the angular velocity of the orbit with respect to the inertial frame; $(I_1, I_2, I_3) = (5, 5.1, 2) kg.m^2$ are the principal moments of inertia of NPSAT1; $\mu = 3.98601 \times 10^{14} m^3/s^2$ is Earth's gravitational constant; $r_0 = 6938 km$ is the distance from the mass center of NPSAT1 to the center of the Earth; $C_{ij}(q)$ denote the quaternion-parameterized ij-th element of the matrix,

$$
C(q) = \begin{bmatrix} q_1^2 - q_2^2 - q_3^2 + q_4^2, & 2(q_1q_2 + q_3q_4), & 2(q_1q_3 - q_2q_4) \\ 2(q_1q_2 - q_3q_4), & q_2^2 - q_1^2 - q_3^2 + q_4^2, & 2(q_2q_3 + q_1q_4) \\ 2(q_1q_3 + q_2q_4), & 2(q_2q_3 - q_1q_4), & q_3^2 - q_1^2 - q_2^2 + q_4^2 \end{bmatrix} \quad \in SO(3)
$$

$(B_x(q,t), B_y(q,t), B_z(q,t))$ are the components of the Earth's magnetic field in the body frame,

$$
\left[B_x(q,t), B_y(q,t), B_z(q,t)\right]^T = C(q)\left[B_1(t), B_2(t), B_3(t)\right]^T
$$

$(B_1(t), B_2(t), B_3(t))$ are the time-varying components of the Earth's magnetic field in the orbit frame,

$$
\begin{aligned}
B_1 &= \frac{M_e}{r_0^3}[\cos(\omega_0 t)[\cos(\epsilon)\sin(i) - \sin(\epsilon)\cos(i)\cos(\omega_e t)] - \sin(\omega_0 t)\sin(\epsilon)\sin(\omega_e t)] \\
B_2 &= -\frac{M_e}{r_0^3}[\cos(\epsilon)\cos(i) + \sin(\epsilon)\sin(i)\cos(\omega_e t)] \\
B_3 &= \frac{2M_e}{r_0^3}[\sin(\omega_0 t)[\cos(\epsilon)\sin(i) - \sin(\epsilon)\cos(i)\cos(\omega_e t)] + 2\cos(\omega_0 t)\sin(\epsilon)\sin(\omega_e t)],
\end{aligned}
$$

where $M_e = 7.943 \times 10^{15} Wb.m$ is the magnetic dipole moment of the Earth, $\epsilon = 11.7^\circ$ is the magnetic dipole tilt, i is the orbit inclination of NPSAT1, $\omega_e = 7.29 \times 10^{-5} rad/s$ is the spin rate of the Earth; see Ref. [29] for further details. The controls, $(u_1, u_2, u_3) \in \mathbb{R}^3$, are the dipole moments on NPSAT1 that are bounded by, $|u_i| \leq 30 A.m^2$, $i = 1, 2, 3$. Clearly, the dynamics of NPSAT1 are quite complex with substantial nonlinearities. Note also that the system is not autonomous. Furthermore, that the quaternions must lie on S^3 is given by the state variable constraint, $q_1^2(t) + q_2^2(t) + q_3^2(t) + q_4^2(t) = 1$. Thus, the NPSAT1 control system contains both state and control constraints.

A benchmark set of endpoint conditions for NPSAT1 are given by,[29]

$$
\begin{aligned}
[q(t_0), \omega(t_0)] &= [0, 0, 0, 1, 0, -0.0011, 0] \\
[q(t_f), \omega(t_f)] &= [\sin(\phi/2), 0, 0, \cos(\phi/2), 0, 7.725 \times 10^{-4}, 7.725 \times 10^{-4}]
\end{aligned}
$$

where $\phi = 135^\circ$ is the principal rotation angle. These endpoint conditions represent a horizon-to-horizon scan. The objective is to find the control that minimizes the slew transfer time.

The problem is solved using both Bellman PS method and the spectral algorithm in Ref. [21]. A comparison of the results are shown in the following figures. Note that, the figures for spectral algorithms are from Ref. [21]. The total number of nodes used there is 292. Due to the high accuracy of spectral algorithm, we regard this solution as the "analytic" optimal solution.

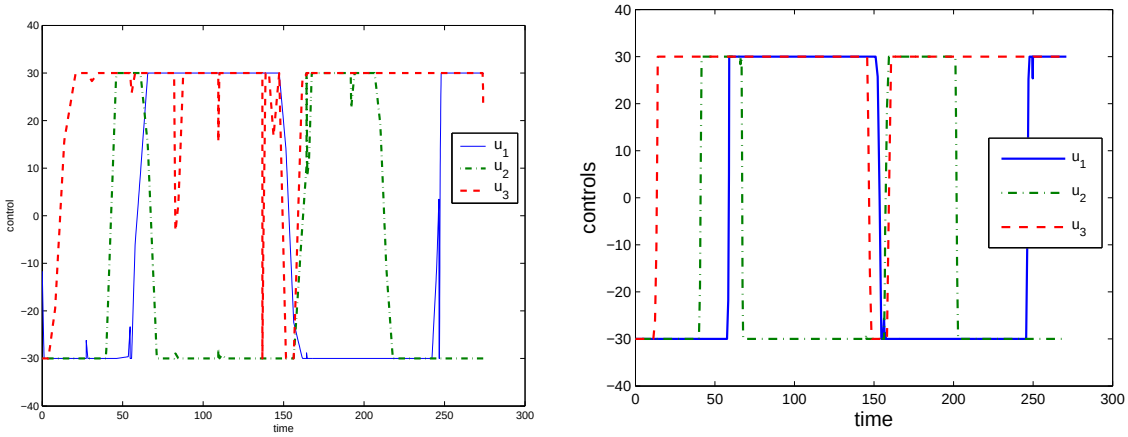

(a) Controls obtained by the Bellman PS approach. (b) Controls obtained by the PS knotting method[20]

Figure 6. Performance comparison — controls.

Applying the proposed Bellman PS method with 30 nodes and 10 segments, the results are shown in the left plot in Fig.6—Fig.8. It can be seen from Fig.6 that, although only 30 nodes are used, the complete control profile resulting from Bellman PS method can still capture the switches relatively accurately.

A comparison of the state trajectories reveals that there are virtually no differences between the Bellman PS trajectories and the "analytic" ones. The final condition errors (defined in the 2-norm) are 7.8967×10^{-5} for quaternions and 5.3313×10^{-6} for angular velocities. This shows that a continuous-time feasible control is indeed obtained by the Bellman PS method with just 30 nodes. Compared to a quaternion error of 0.01351 and a velocity error of 8.741×10^{-5} for 30 nodes without using Bellman PS algorithm, the performance improvement is quite apparent.

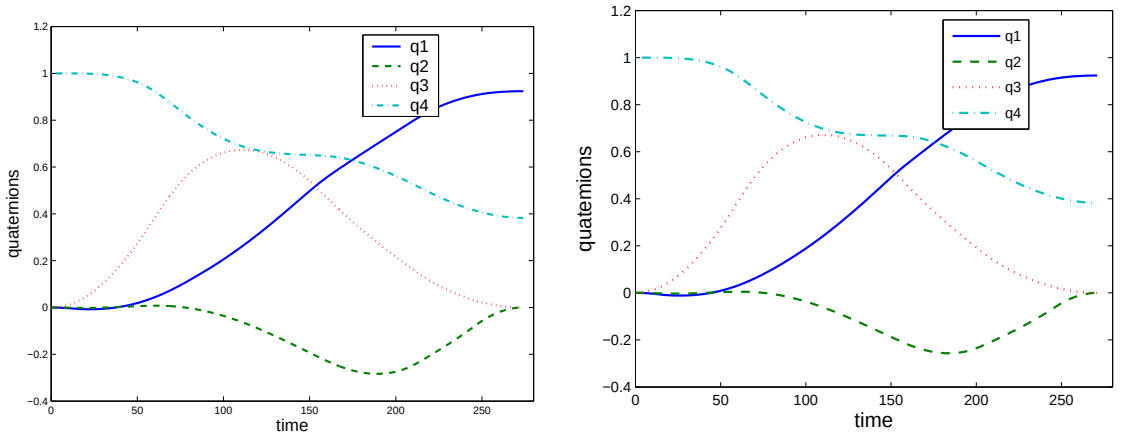

(a) Quaternions obtained by the Bellman PS approach. (b) Quaternions obtained by the PS knotting method[20]

Figure 7. Performance comparison — quaternions.

The minimum time need to complete the maneuver using the Bellman PS algorithm was 274.0 seconds. Compared to the "analytic" solution of 272.4 seconds, the performance loss is a mere 0.6%.

VI. Conclusions

A low cost computational algorithm is proposed to improve the feasibility of a solution in solving optimal control problems. The algorithm combines the good properties of pseudospectral methods with an intuitive

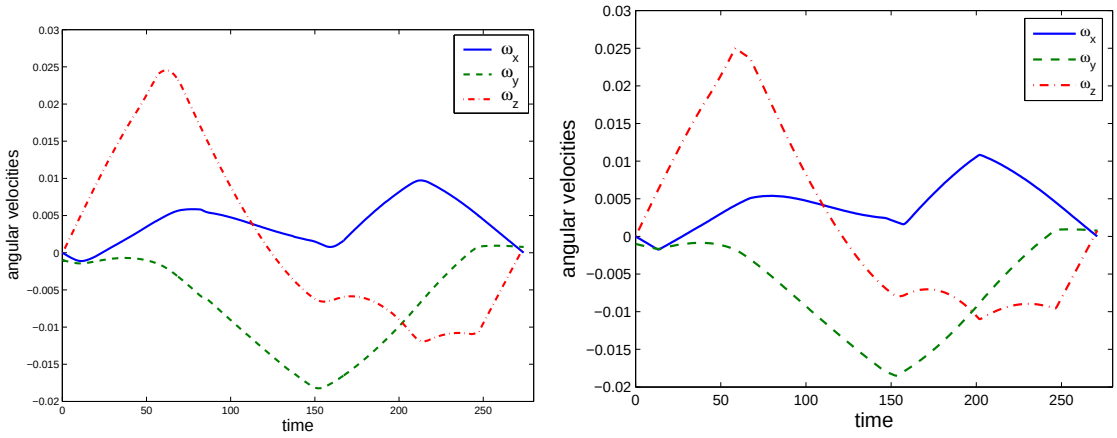

(a) Velocities obtained by the Bellman PS approach.

(b) Velocities obtained by the PS knotting method[20]

Figure 8. Performance comparison — velocities.

idea borrowed from Bellman. By propagating the control and repeatedly solving the optimal control problem, the algorithm guarantees practical continuous-time feasibility at very low computational cost. This algorithm can also be incorporated into a closed-loop structure to provide real-time online solutions for optimal control applications.

References

[1]Kang, W. and Bedrossian, N., "Pseudospectral Optimal Control Theory Makes Debut Flight," *SIAM News, Volume 40, Number 7, September 2007.*

[2]Group Projects in Space Propulsion, http://trajectory.grc.nasa.gov/projects/lowthrust.shtml.

[3]Ross, I. M., User's manual for DIDO: A MATLAB application package for solving optimal control problems, Elissar, Monterey, CA, 2007.

[4]Infeld, S. I., "Optimization of Mission Design For Constrained Libration Point Missions," Ph.D. Dissertation, Department of Aeronautics and Astronautics, Stanford University, December 2005.

[5]Lu, P., Sun H., and Tsai, B., "Closed-Loop Endoatmospheric Ascent Guidance," *Journal of Guidance, Control and Dynamics*, Vol. 26, No. 2, pp.283-294, 2003.

[6]Melton, R. G., "Comparision of Direct Optimization Mehods Applied to Solar Sails," *AIAA/AAS Astrodynamics Specialists Conference and Exhibit*, 5-8 August 2002, Monterey, CA, AIAA 2002-4728.

[7]Paris, S. W., Riehl, J. P. and Sjaw, W. K., "Enhanced Procedures for Direct Trajectory Optimization Using Nonlinear Programming and Implicit Integration," AIAA/AAS Astodynamics Specialist Conference and Exhibit, 21-24 August 2006, Keystone, CO, AIAA 2006-6309.

[8]Riehl, J. P., Paris, S. W., and Sjaw, W. K., "Comparision of Implicit Integration Methods for Solving Aerospace Trajectory Optimization Problems," AIAA/AAS Astodynamics Specialist Conference and Exhibit, 21-24 August 2006, Keystone, CO, AIAA 2006-6033.

[9]Harada, M., and Bollino, K., "Optimal Trajectory of a Glider in Ground Effect and Wind Shear," *AIAA Guidance, Navigation and Control Conference*, San Francisco, CA, August 15-18, 2005. AIAA 2005-6474.

[10]Hawkins, A. M., Fill, T. R., Proulx, R. J., Feron, E. M., "Constrained Trajectory Optimization for Lunar Landing," *AAS Spaceflight Mechanics Meeting*, Tampa, FL, January 2006, AAS 06-153.

[11]Infeld, S. I. and Murray, W., "Optimization of Stationkeeping for a Libration Point Mission," *AAS Spaceflight Mechanics Meeting*, Maui, HI, February 2004. AAS 04-150.

[12]J. Pietz and N. Bedrossian, "Moemtum Dumping Using Only CMGs," *Proceedings of the AIAA GNC Conference*, Austin, TX, 2003.

[13]Rea, J., "Launch Vehicle Trajectory Optimization Using a Legendre Pseudospectral Method," *Proceedings of the AIAA Guidance, Navigation and Control Conference*, Austin, TX, August 2003. Paper No. AIAA 2003-5640.

[14]S. Stanton, R. Proulx and C. D'Souza, Optimal orbit transfer using a Legendre pseudospectral method, *AAS/AIAA Astrodynamics Specialist Conference*, AAS-03-574, Big Sky, MT, August 3-7, 2003.

[15]P. Williams, Application of Pseudospectral Methods for Receding Horizon Control, *J. of Guid., Contr. and Dyn.*, Vol.27, No.2., 2004, pp.310-314.

[16]P. Williams, C. Blanksby and P. Trivailo, Receding horizon control of tether system using quasilinearization and Chebyshev pseudospectral approximations, *AAS/AIAA Astrodynamics Specialist Conference*, Big Sky, MT, August 3-7, 2003, Paper AAS 03-535.

[17]H. Yan and K. T. Alfriend, Three-axis Magnetic Attitude Control Using Pseudospectral Control Law in Eccentric Orbits, *AAS Spaceflight Mechanics Meeting*, Tampa, FL, January 2006, AAS 06-103.

[18]Ross, I. M., Sekhavat, P., Fleming, A., and Gong, Q., Optimal feedback control: foundations, examples, and experimental results for a new approach, *AIAA Journal of Guidance, Control, and Dynamics*, vol. 31 no. 2, pp. 307-321, 2008.

[19]Ross, I. M., Gong, Q., Fahroo, F., and Kang, W., Practical stabilization through real-time optimal control, *Proc. of American Control Conference*, pp. 304-309, Minneapolis, MN, June, 2006.
[20]Gong, Q., Fahroo, F. and Ross, I. M., A spectral algorithm for pseudospectral methods in optimal control, *AIAA Journal of Guidance, Control and Dynamics,* Vol. 31, No. 3, pp. 460-471, 2008.
[21]Ross, I. M., Gong, Q. and Sekhavat, P., "Low-Thrust, High-Accuracy Trajectory Optimization," *Journal of Guidance Control and Dynamics*, Vol. 30, No. 4, July-August 2007, pp. 921-933.
[22]Ross, I. M., and Fahroo, F., "Pseudospectral Knotting Methods for Solving Optimal Control Problems," *Journal of Guidance, Control and Dynamics*, Vol. 27, No. 3, pp. 397-405, 2004.
[23]Canuto, C., Hussaini, M. Y., Quarteroni, A., and Zang, T. A., *Spectral Methods in Fluid Dynamics,* Springer Verlag, New York, 1988.
[24]Trefethen, L. N., *Spectral Methods in MATLAB,* SIAM, Philadelphia, PA, 2000.
[25]Gong, Q., Kang, W. and Ross, I. M., A pseudospectral method for the optimal control of constrained feedback linearizable systems, *IEEE Trans. on Automatic Control*, Vol. 51, No. 7, July 2006, pp. 1115-1129.
[26]Gong, Q., Ross, I. M., Kang, W. and Fahroo, F., On the pseudospectral covector mapping theorem for nonlinear optimal control, *IEEE Conf. on Decision and Control*, pp. 2679-2686, San Diago, CA, Dec. 2006.
[27]Gong, Q., Ross, I. M., Kang, W. and Fahroo, F., Connections between the covector mapping theorem and convergence of pseudospectral methods for optimal control, to appear in *Computational Optimization and Applications*, 2008.
[28]Polak, E., *Optimization: Algorithms and Consistent Approximations*, Springer-Verlag, Heidelberg, 1997.
[29]Fleming, A., Real-time optimal slew maneuver design and control, Astronautical Engineer's Thesis, US Naval Postgraduate School, December 2004.